Proceedings of the Sixth International Conference on
Railway Technology: Research, Development and Maintenance
Edited by: J. Pombo
Civil-Comp Conferences, Volume 7, Paper 24.4
Civil-Comp Press, Edinburgh, United Kingdom, 2024
ISSN: 2753-3239, doi: 10.4203/ccc.7.24.4

DEM Analysis of Lateral Sleeper Resistance: Effect of Sleeper-Ballast Interaction and Aggregate Friction

C. Shi[1,2], A. Andersson[1], L. Xu[3] and J. Guo[4]

**[1]Department of Civil and Architectural Engineering
KTH Royal Institute of Technology, Stockholm, Sweden
[2]College Civil and Transportation Engineering,
Shenzhen University, Shenzhen, China
[3]School of Civil Engineering, Central South University
Changsha, China
[4]Department of Engineering Mechanics,
KTH Royal Institute of Technology, Sweden**

Abstract

This study utilizes a 3D DEM sleeper-ballast bed model, comprising four sleepers interacting with the actual shape of the ballast, to comprehensively explore the impact of sleeper-ballast interaction and ballast aggregate friction coefficient on the lateral resistance of ballast bed. Based on the DEM numerical simulation, the following conclusion can be drawn: 1) The friction resistance between the sleeper and the ballast is crucial in determining the lateral resistance in railway tracks, with the base ballast contributing to more than 50% of the lateral resistance of the ballast bed on average; 2) The sleeper bottom resistance and sleeper side resistance of lateral force is derived from the sleeper-ballast friction mechanisms, while the friction coefficient between the sleeper end and the shoulder ballast has minimal impact on the sleeper end resistance; 3) The lateral resistance of the ballast bed is more significantly influenced by alterations in the ballast friction coefficient than by changes in the friction coefficient sleeper-ballast interface.

Keywords: railway ballasted track, lateral resistance, discrete element method, ballast bed, friction coefficient, sleeper-ballast interaction

1 Introduction

The stability of the track is crucial for ensuring normal railway transportation and operational safety. It is closely related to factors such as train loads, the fastening system, sleeper geometry, type and weight of sleepers, type of ballast, the thickness and consolidation of the ballast layer, and maintenance services. Currently, track stability is fundamentally assessed by the index of track lateral resistance, which is essentially considered to be influenced by the ballast, the fastening system, and rails, with contributions of 60%, 30%, and 10%, respectively [1]. The lateral resistance of the ballast bed, referred to here as lateral sleeper resistance, constitutes the main part of track lateral resistance. It primarily associated with the interface between the ballast and sleepers, specifically located at the sleeper bottom (base ballast), the sleeper side (crib ballast), and the sleeper end (shoulder ballast), as illustrated in Figure 1.

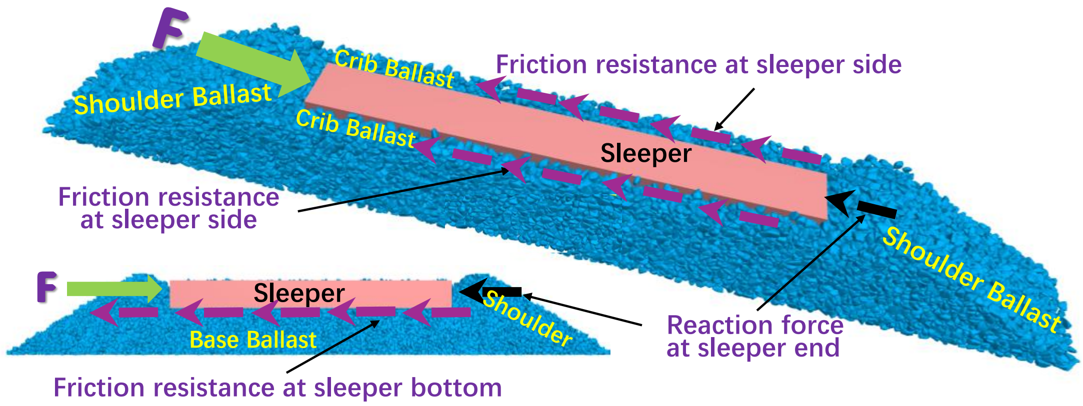

Figure 1: Components of lateral sleeper resistance

In particular, the resistance offered by the base ballast is dependent on the vertical load, whereas that related to the crib and shoulder is essentially related to the internal friction of the ballast and the volume of the grains involved by the sleepers' movements [2]. The resistance contributions offered by the base, the crib, and the shoulder to the total resistance of the ballast bed have been identified in Ref. [3-6], and all studies showed a minimum contribution of 60%-70% for both base and crib zones with the friction mechanisms between the sleeper and ballast. Therefore, the influence of interaction friction between sleeper and ballast on resistance of the sleeper requires specially attention.

Based on the experimental research, Lichtberger [7] indicated that ballast consolidation within the sleeper cribs enhances resistance to lateral displacement by approximately 7%, consolidation at the sleeper ends contributes a 4% increase, while the dynamic track stabilizer augmenting resistance to lateral displacement by 30-40%. Mechanical stabilization following surfacing has been demonstrated as the most effective method, as evidenced in Ref. [8] across all tested sections. Besides, Zakeri and Mirfattahi [9] founded that the lateral resistance of the railway track increases by approximately 67% with the use of simple mono-block concrete ties instead of friction concrete ties. Furthermore, the results of experimental research activities on the sleeper–ballast resistance along the lateral directions are reported and discussed in [10-11].

Generally, these experimental studies reveal the friction interaction between sleepers and ballast have a significant influence on the lateral resistance of the sleeper. However, it is challenging for experimental research to control the initial contact state between the sleeper and ballast for a series of tests. Additionally, experimental studies face difficulties in directly or indirectly measuring the frictional contributions of different parts of the sleepers to the lateral resistance of ballast bed. Therefore, experimental studies struggle to statistically quantify the contribution of friction interactions between sleepers and ballast to the overall lateral resistance.

In recent years, with the widespread adoption of discrete element methods (DEM) in ballast simulation [12-14], scholars have commonly employed DEM simulations to further investigate the track resistance characteristic. Such as, Liu et al. [15] compared the resistances of composite and concrete sleepers in ballast beds and obtained that lateral resistance of the composite sleeper is about 36% lower than that of the concrete sleeper with an increase in displacement at 2 mm. Jing et al. [16] obtained that applying the arrowhead groove frictional sleeper is able to improve lateral resistance by 7–24%. Guo et al. [17] indicated that the frictional sleepers can increase the lateral resistance by 32% (maximum), due to the enhanced interaction between sleeper and ballast particles. Esmaeili et al. [18] introduced a ‘‘nailed sleeper” for enhancing the lateral resistance of concrete sleepers and observed that using a pair of nails of 40 mm in diameter and 1500 mm in length can increase the lateral resistance more than 200% compared to the normal condition. Besides, Hosseini et al. [19] investigated the interaction between different surfaces (base, crib, and shoulder) of concrete sleeper under lateral impact loading condition.

The above studies quantified the influence of ballast-sleeper interaction on the lateral resistance of the sleeper in ballasted track. Since the changing of the ballast states can alter the ballast-sleeper friction resistance, scholars have also further investigated the influence of the ballast particles on the lateral resistance of the ballast bed. Ngamkhanong et al. [20] evaluated ballasted track lateral resistance considering different fouling scenarios and indicated that fouled ballast can significantly undermine the lateral stability of ballasted tracks by more than about 50%. Esmaeili et al. [21-22] obtained that a 27% increase in lateral resistance of track with steel slag ballast respect to that with limestone ballast, and the lateral resistance of the common ballasted track is about 55–80% more than that of the ballasted track with full-depth hot mix asphalt. Besides, Woodward et al. [23], Ling et al. [24] and Xiao et al. [25] displayed that the lateral resistance of the ballast bed could be increased to more than three times the normal values by bonding the ballast particles.

In summary, the above studies investigated the influence of different types of sleepers and ballast layer conditions on the lateral resistance of ballast bed. Studies specific to certain track types have specific and clear research significance. However, due to the poor consistency in initial contact states between sleepers and ballast, this paper considers the sleeper-ballast contact status as changes in friction coefficient. Further quantitative research is conducted on the characteristics of the sleeper-ballast contact status affecting the lateral resistance of the ballast bed, aiming to provide more universal and general conclusions. Firstly, the DEM model of the sleeper-ballast bed is introduced and described. Then, the effects of changes in the friction coefficient at the bottom of the sleeper, the friction coefficient at the bottom and surrounding areas of the sleeper, and the friction coefficient of the ballast particles on the lateral resistance of ballast bed were investigated separately.

2 3D DEM model of the sleeper-ballast bed

2.1 A description of the sleeper-ballast bed DEM model

Figure 2 shows the 3D DEM model of sleeper and ballast bed used in this work. The model has a length of 2.4 m along the track direction including 4 sleepers, named from nearest to furthest as No. 1 sleeper to No. 4 sleeper, with a spacing of 0.6 m between each sleeper. For more details about the modelling process can be further referred to Ref. [26]. Note that, since this paper primarily focuses on investigating the lateral resistance characteristics of the ballast to sleeper lateral movement, the DEM model in this work does not take the rail and fastening system into consideration.

The thickness of the ballast bed is 0.35 m, the top width of the ballast bed is 3.6 m, the slope of the ballast bed is 1:1.75, and the distance between sleepers No. 1 and No. 4 and the boundary wall is 0.3 m. In this DEM model, a linear contact model [27] is adopted to simulate the interaction behaviour between sleeper and ballast bed. The contact model parameters used in this study are consistent with those reported in other studies [28, 29]. Specifically, the friction coefficient between the ballast particles and the sleeper is set at 0.5, and the friction coefficient between the ballast and the wall units is also 0.5.

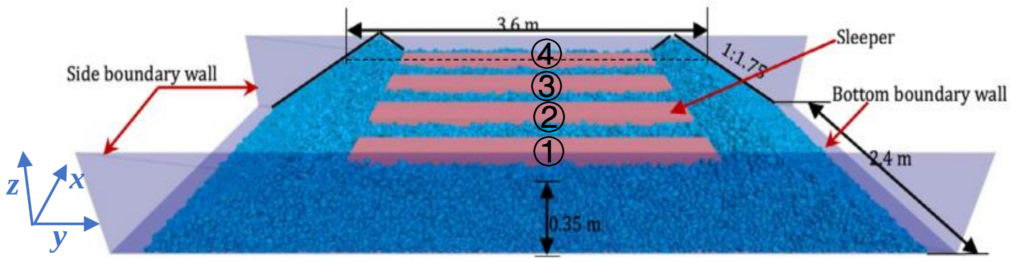

Figure 2: The 3D DEM model of sleeper and ballast bed.

2.2 Validation of the sleeper-ballast bed DEM model

In the DEM simulation, a concentrated force is applied to individual sleepers in the x-direction, and their resulting lateral displacement is recorded. The lateral resistance of the ballast bed is determined when the lateral displacement of the sleepers reaches 2mm. This process is repeated sequentially for each sleeper, enabling the characterization of the lateral resistance properties of the ballast bed across all four sleepers.

Figure 3 shows the relationship between the applied force and the sleeper displacement for four sleepers. Figure 3 indicate consistent trends in the lateral resistance of the ballast bed across all sleepers, and the value of lateral resistance of ballast bed is 19.3 kN, 14.3 kN, 15.4 kN, 18.6 kN for four sleepers when the sleeper displacement reaches 2 mm. This meet the requirement of Chinese standard, with the minimum limit value of lateral resistance of ballast bed is 12 kN/sleeper [30-31]. The range of simulation values are covered by the measured values of 13 – 22 kN/sleeper in Ref. [8] for well-compacted ballast beds. Therefore, the correctness of the DEM model simulating the lateral resistance of the ballast bed has been validated.

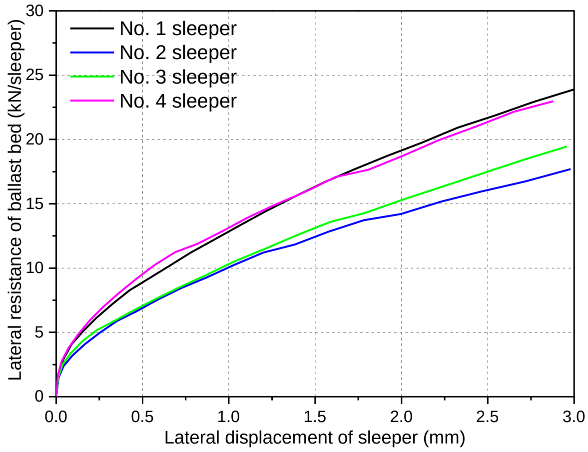

Figure 3: Relationship between the lateral force and displacement of sleeper.

3 Analysis of the lateral resistance of the ballast bed with different friction coefficients

To thoroughly investigate the influence of the friction coefficient of various components and interactions within the sleeper-ballast bed on the lateral resistance of the ballast bed, the friction coefficient at the interface between the sleeper bottom and the ballast is examined in Section 3.1, while the friction coefficient of the sleeper is focused on in Section 3.2. Section 3.3 investigates the friction coefficient of the ballast particles. Table 1 lists set for the sleeper-ballast interface and components in this study. the selected values for the friction coefficient settings of the parameters are 0.3, 0.5, 0.7 and 0.9, based on the typical range of friction coefficients for ballast particles, which typically range from 0.3 to 0.9 according to DEM simulation [32-36].

Parameter settings for different components	Variation friction coefficient at the bottom of sleepers				Variation friction coefficient of sleepers				Variation Friction coefficient of ballast			
	0.3	0.5	0.7	0.9	0.3	0.5	0.7	0.9	0.3	0.5	0.7	0.9
At the bottom of sleepers	0.3	0.5	0.7	0.9	0.3	0.5	0.7	0.9	0.3	0.5	0.7	0.9
At the side of sleepers	0.5	0.5	0.5	0.5	0.3	0.5	0.7	0.9	0.3	0.5	0.7	0.9
At the end sleepers	0.5	0.5	0.5	0.5	0.3	0.5	0.7	0.9	0.3	0.5	0.7	0.9
For the ballast particles	0.5	0.5	0.5	0.5	0.5	0.5	0.5	0.5	0.3	0.5	0.7	0.9
For the wall elements	0.5	0.5	0.5	0.5	0.5	0.5	0.5	0.5	0.5	0.5	0.5	0.5

Table 1: Setting the friction coefficient for sleeper-ballast interface and component

3.1 Influence of friction coefficient at the bottom of sleeper on the lateral resistance

Figure 4 illustrates the relationship between the lateral resistance of ballast bed and the different friction coefficients at the bottom of sleeper. Each point in the graph represents the lateral resistance value of the ballast bed corresponding to the friction coefficient at the bottom of each sleeper. From Figure 4, the lateral resistance of the ballast bed increases as the friction coefficient at the interface between the sleeper bottom and the ballast increases. The trend appears to exhibit an exponential growth as the friction coefficient increases from 0.3 to 0.9, indicating a significant acceleration in the rate of increase in the lateral resistance of the ballast bed.

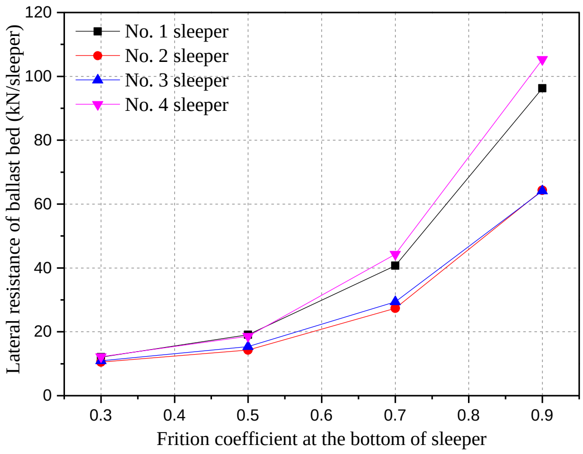

Figure 4: Lateral resistance of ballast bed under different friction coefficients at the interface between the sleeper bottom and the ballast.

Figure 5 illustrates the contribution of ballast at different parts around No. 3 sleeper to the lateral resistance of the ballast bed. Figure 5(a) shows that the lateral resistance provided by the ballast beneath the sleeper increases linearly as the lateral displacement of the sleeper increases. The same trend is evident across different friction coefficient conditions. In Figure 5(b), it is shows that the lateral resistance provided by the shoulder ballast initially increases significantly with the sleeper's lateral displacement and then stabilizes, remaining constant at around 1 kN. This contributes a relatively small proportion to the overall lateral resistance of the ballast bed. For the ballast in the cribs on both sides of the sleeper, Figures 5(b) and 5(c) indicate that as the lateral displacement of the sleeper increases, the lateral resistance provided by the crib ballast initially increases significantly, followed by a reduced rate of increase.

Furthermore, Figure 5(a)-(c) indicate that with the increase of the friction coefficient, the lateral resistance provided by the ballast at the bottom of the sleeper increases, while the lateral resistance provided by the ballast at the shoulder of the sleeper and on both sides of the crib decreases. This is mainly due to the increase in the friction coefficient at the bottom of the sleeper, which causes the ballast at the bottom of the sleeper to bear more lateral resistance. Consequently, this reduces the contribution of ballast at other positions of the sleeper to the lateral resistance during the lateral displacement of the sleeper.

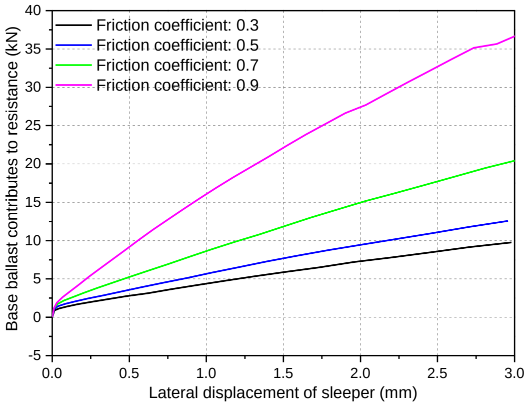

(a) Base ballast contribution

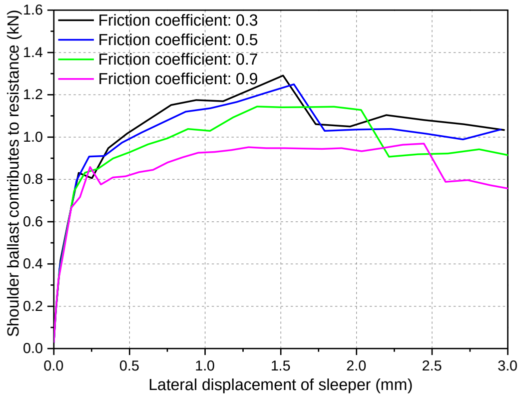

(b) Shoulder ballast contribution

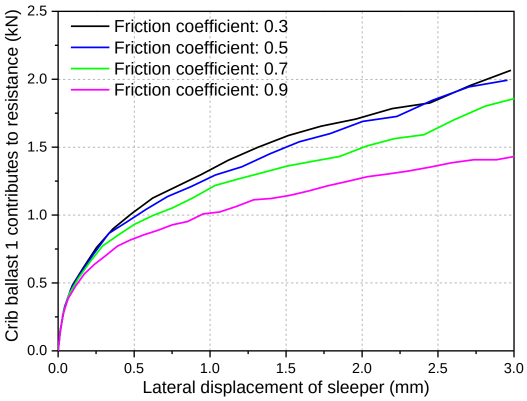

(c) Crib 1 ballast contribution

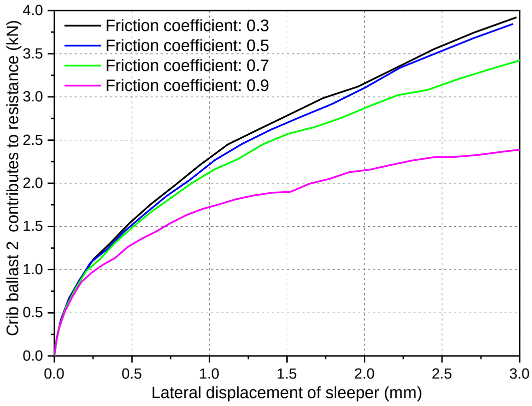

(d) Crib 2 ballast contribution

Figure 5: Contribution of ballast at different part of sleeper to lateral resistance with different friction coefficients at the bottom of sleeper.

Table 2 summarizes the lateral resistance of the ballast bed and the lateral resistance provided by the ballast at bottom of the sleeper. It also lists the contribution percentage of base ballast to the lateral resistance of the sleeper. Table 2 indicates that with a friction coefficient of 0.5 at the bottom of the sleeper, the lateral resistance of the ballast bed fluctuates between 14.3 and 19.3 kN per sleeper. The contribution percentage of base ballast to the lateral resistance of the sleeper ranges from 50.8% to 63.6%, with an average of 57.9%. This range aligns with the measured results of 37%-62% reported in references [37-38].

Furthermore, from Table 2, it can be observed that as the friction coefficient increases, the proportion of the lateral resistance provided by the bottom of the sleeper to the total lateral resistance of the ballast bed also increases. When the friction coefficient at the bottom of the sleeper increases from 0.3 to 0.9, the average lateral resistance provided by the bottom ballast increases from 6.7 kN to 32.2 kN, along with an increase in the proportion of the lateral resistance contributed by the bottom of the sleeper to the total lateral resistance of the ballast bed from 47.8% to 85.6%. Meanwhile, the lateral resistance value of the ballast bed increases from 14.1 kN/sleeper to 37.7 kN/sleeper. Therefore, it can be concluded that increasing the friction coefficient at the bottom of the sleeper can effectively increase the lateral resistance provided by the bottom ballast and enhance the overall lateral resistance of the ballast bed.

	Lateral resistance with friction coefficient of 0.3			Lateral resistance with friction coefficient of 0.5			Lateral resistance with friction coefficient of 0.7			Lateral resistance with friction coefficient of 0.9		
	Base	Total	Percentage	Base	Total	Percentage	Base	Total	Percentage	Base	Total	Percentage
No.1	5.7	15.5	36.8%	9.8	19.3	50.8%	23.1	30.9	74.8%	38.6	45.7	84.5%
No.2	7.6	12.9	58.9%	9.1	14.3	63.6%	15.5	19.9	77.9%	23.9	27.8	86.0%
No.3	7.3	13.3	54.9%	9.5	15.4	61.7%	14.9	20.5	72.7%	27.4	31.7	86.4%
No.4	6.0	14.8	40.5%	10.3	18.6	55.4%	21.2	28.6	74.1%	39.0	45.5	85.7%
Avg.	**6.7**	**14.1**	**47.8%**	**9.7**	**16.9**	**57.9%**	**18.7**	**25.0**	**74.9%**	**32.2**	**37.7**	**85.6%**

Table 2: Base ballast contributes to the percentage of lateral resistance with different friction coefficients at the bottom of sleeper.

3.2 Influence of friction coefficient of sleeper on the lateral resistance

Table 3 further summarizes the values of the lateral resistance provided by the ballast at different parts of the sleeper when the sleeper moves laterally by 2 mm. From Table 3, as the friction coefficient of the sleeper increases, the lateral resistance provided by the ballast at the bottom of the sleeper and on both sides of the crib increases, while the lateral resistance provided by the ballast at the end of the sleeper decreases. This further proved that the main contribution of the ballast at the bottom of the sleeper and on both sides of the crib to the lateral resistance of the ballast bed is provided by the friction interaction between the sleeper and the ballast. Conversely, the contribution of the ballast at the shoulder of the sleeper to the lateral resistance of the ballast is minimally affected by the friction interaction between the sleeper end and the shoulder ballast.

	Lateral resistance with friction coefficient of 0.3			Lateral resistance with friction coefficient of 0.5			Lateral resistance with friction coefficient of 0.7			Lateral resistance with friction coefficient of 0.9		
	Bottom	Shoulder	Crib	Bottom	Shoulder	Crib	Bottom	Shoulder	Crib	Bottom	Shoulder	Crib
No.1	6.4	4.5	4.4	10.0	4.0	5.1	23.4	3.3	5.7	35.9	2.8	9.4
No.2	8.2	0.7	3.8	9.2	0.6	4.4	14.9	0.47	4.5	24.2	0.45	4.9
No.3	7.7	1.2	3.9	9.5	1.0	4.9	14.4	1.2	4.9	26.8	0.9	5.8
No.4	6.9	2.6	4.5	10.3	2.3	6.2	21.3	1.7	9.9	37.6	1.6	11.4
Avg.	**7.3**	**2.3**	**4.2**	**9.8**	**2.0**	**5.2**	**18.5**	**1.7**	**6.3**	**31.1**	**1.4**	**7.9**

Table 3: Contribution value of ballast at different part of sleeper to lateral resistance with different friction coefficients of sleeper.

Table 4 lists the lateral resistance values of the ballast bed for sleepers under different sleeper friction coefficients. The lateral resistance average values of the ballast bed are 13.7 kN/sleeper, 16.9 kN/sleeper, 26.4 kN/sleeper, and 40.4 kN/sleeper when the sleeper friction coefficients are 0.3, 0.5, 0.7, and 0.9, respectively. When the friction coefficient of the sleeper is 0.9, the proportion of lateral resistance provided by the base ballast of the sleeper is approximately 77.0%. This is slightly reduced compared to the 85.6% proportion of lateral resistance provided by the base ballast of the sleeper with a friction coefficient of 0.9 in Table 2 of Section 3.1. This reduction is mainly due to the increased friction resistance provided by the crib ballast when the friction coefficient of the sleeper is 0.9, causing a slight decrease in the proportion of lateral resistance provided by the base ballast of the sleeper. This also indicates the variations of friction coefficient between the ballast and sleepers significantly impact the proportion results of the lateral resistance contributed by the ballast at different interfaces around the sleepers.

	Lateral resistance with friction coefficient of 0.3			Lateral resistance with friction coefficient of 0.5			Lateral resistance with friction coefficient of 0.7			Lateral resistance with friction coefficient of 0.9		
	Base	Total	Percentage	Base	Total	Percentage	Base	Total	Percentage	Base	Total	Percentage
No.1	6.4	15.3	41.8%	9.8	19.3	50.8%	23.4	32.4	72.2%	35.9	48.1	74.6%
No.2	8.2	12.7	64.6%	9.1	14.3	63.6%	14.9	19.9	74.9%	24.2	29.5	82.0%
No.3	7.7	12.8	60.2%	9.5	15.4	61.7%	14.4	20.5	70.2%	26.8	33.5	80.0%
No.4	6.9	14.0	49.3%	10.3	18.6	55.4%	21.3	32.9	64.7%	37.6	50.6	74.3%
Avg.	**7.3**	**13.7**	**53.3%**	**9.66**	**16.9**	**57.9%**	**18.5**	**26.4**	**70.0%**	**31.1**	**40.4**	**77.0%**

Table 4: Base ballast contributes to the percentage of lateral resistance with different friction coefficients of sleepers.

3.3 Influence of friction coefficient of ballast particle on the lateral resistance

Table 5 lists the values of lateral resistance provided by the ballast at different parts of the sleeper under different ballast friction coefficient conditions. From Table 5, it can be observed that with the increase in ballast friction coefficient, the lateral resistance provided by the base ballast, crib ballast, and shoulder ballast of the sleeper all increase. Interestingly, the increase in ballast friction coefficient also leads to an increase in the friction coefficient provided by the shoulder ballast, contrary to the trend observed in Table 3 regarding the increase of sleeper friction coefficient. This is primarily due to the greater interlocking friction between the end crib ballast as the ballast friction coefficient increases, resulting in better overall integrity of the shoulder ballast and thus providing greater lateral resistance to the ballast bed.

Additionally, from Table 5, it is evident that the lateral resistance provided by the shoulder ballast is significantly smaller compared to other sections under different ballast friction coefficient conditions. When the ballast friction coefficient is 0.9, the friction resistance provided by the base ballast, shoulder, and crib ballast increases by 135%, 48%, and 149%, respectively, compared to when the ballast friction coefficient is 0.7. This indicates that the shoulder ballast has a limited effect on enhancing lateral resistance, while the crib ballast exhibits the greatest increase. Therefore, when employing methods such as ballast bonding to enhance the lateral resistance of existing ballast bed, it is advisable to focus on bonding the crib section of the ballast.

	Lateral resistance with friction coefficient of 0.3			Lateral resistance with friction coefficient of 0.5			Lateral resistance with friction coefficient of 0.7			Lateral resistance with friction coefficient of 0.9		
	Bottom	Shoulder	Crib	Bottom	Shoulder	Crib	Bottom	Shoulder	Crib	Bottom	Shoulder	Crib
No.1	6.3	2.4	3.4	10.0	4.0	5.1	23.9	6.5	10.2	54.1	8.2	33.8
No.2	6.4	0.6	3.4	9.2	0.56	4.44	19.7	0.5	6.9	50.4	0.8	12.7
No.3	6.1	1.1	3.6	9.5	1.0	4.9	21.4	1.0	7	48.3	1.4	14.1
No.4	6.4	1.8	4.1	10.3	2.3	6.2	23.9	2.9	17.7	55.7	5.7	43.2
Avg.	6.3	1.5	3.6	9.8	2.0	5.2	22.2	2.7	10.5	52.1	4.0	26.0

Table 5: Contribution value of ballast at different part of sleeper to lateral resistance with different friction coefficients of ballasts.

Figure 6 compares the lateral resistance of ballast bed with different friction coefficients for the sleeper bottom, the sleeper and the ballast. From Figure 6, it can be observed that the average lateral resistance of the ballast bed under a ballast friction coefficient of 0.9 is 82.1 kN/sleeper, which is significantly larger compared to 37.68 kN/sleeper and 40.43 kN/sleeper when the friction coefficient of the sleeper and the base of the sleeper is 0.9, respectively. This is mainly due to the increased friction coefficient between the ballast particles, which enhances the interlocking effect between them, thereby improving the overall integrity of the ballast bed and significantly increasing its lateral resistance. Moreover, when the ballast friction coefficient is 0.3, the lateral resistance of the ballast bed is lower than when the sleeper friction coefficient is 0.3, suggesting a larger reduction in lateral resistance as the ballast bed deteriorates. In summary, changes in the ballast friction coefficient have a more pronounced effect on the lateral resistance of the ballast bed compared to changes in the sleeper friction coefficient.

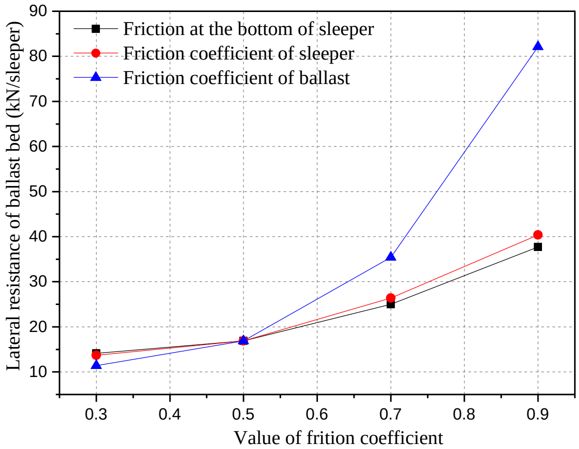

Figure 6: Lateral resistance of ballast bed with different friction coefficients for sleeper-ballast interface and component.

4 Conclusions and contributions

This work utilizes a 3D DEM of sleeper-ballast bed to study the lateral resistance of the ballast bed with different friction coefficients of ballast aggregate and sleeper-ballast interaction.

Considering that friction sleeper designs usually modify the structure of the bottom to increase friction, the first part of this work investigates the influence of changing the friction coefficient at the contact between the sleeper bottom and the ballast on the lateral resistance. Based on the numerical simulation conducted in this study, the base ballast contributes between 50.8% and 63.6% to the lateral resistance of the sleeper, with an average contribution of 57.9%. Additionally, the results indicate that increasing the friction coefficient at the bottom of the sleeper can effectively enhance the lateral resistance.

By exploring the effect of altering the friction coefficient around the sleeper on the lateral resistance of the sleeper, the simulation results prove that the sleeper bottom resistance and sleeper side resistance of lateral force is derived from the sleeper-ballast friction mechanisms, while the friction between the sleeper end and the shoulder ballast has minimal impact on the sleeper end resistance. Besides, the results also indicate that the variations in the friction coefficient between the ballast and the sleeper significantly impact the proportion of the lateral resistance contributions from the different positions of sleeper-ballast interface.

Finally, given friction coefficients depends on the materials, degradation and gradations of ballast particle, the impact of changes in the surface friction coefficient of ballast particle on the lateral resistance of the sleeper is examined. The DEM simulation results indicate that changes in the ballast friction coefficient have a more substantial impact on the lateral resistance of the ballast bed compared to alterations in the friction coefficient at the sleeper-ballast interface. Furthermore, increasing the ballast friction coefficient significantly boosts the contribution of lateral resistance from the crib ballast. Therefore, for existing ballasted tracks, it is advisable to prioritize bonding the crib section to enhance lateral resistance when using methods like ballast bonding.

Acknowledgements

This work was supported by the National Key Research and Development Program of China under grant 2022YFB2603300.

References

[1] De Iorio, A., Grasso, M., Penta, F., Pucillo, G. P., & Rosiello, V. (2014). Transverse strength of railway tracks: part 2. Test system for ballast resistance in line measurement. Frattura ed Integrità Strutturale, 8(30), 578-592.

[2] Kish A (2011). On the fundamentals of track lateral resistance. In: AREMA annual conference.

[3] Le Pen LM and Powrie W (2011). Contribution of base, crib, and shoulder ballast to the lateral sliding resistance of railway track: A geotechnical perspective. Proc IMechE, Part F: J Rail and Rapid Transit; 225: 113–128.

[4] Khatibi, F., Esmaeili, M., & Mohammadzadeh, S. (2017). DEM analysis of railway track lateral resistance. Soils and foundations, 57(4), 587-602.

[5] Aela, P., Zong, L., Powrie, W., & Jing, G. (2023). Influence of ballast shoulder width and track superelevation on the lateral resistance of a monoblock sleeper using discrete element method. Transportation Geotechnics, 42, 101040.
[6] Khatibi, F., Esmaeili, M., & Mohammadzadeh, S. (2017). DEM analysis of railway track lateral resistance. Soils and foundations, 57(4), 587-602.
[7] Lichtberger, B. (2007). The lateral resistance of the track (Part 2). European Railway Review.
[8] Sussmann, T., Kish, A., & Trosino, M. (2003). Influence of track maintenance on lateral resistance of concrete-tie track. Transportation research record, 1825(1), 56-63.
[9] Zakeri, J. A., & Mirfattahi, B. (2020). Field investigation on the lateral resistance of railway tracks with frictional sleepers. In IOP Conference Series: Materials Science and Engineering (Vol. 671, No. 1, p. 012125). IOP Publishing.
[10] Ichikawa, T., Hayano, K., Nakamura, T., & Momoya, Y. (2016). Lateral resistance of ballasted tracks for various shapes of sleepers based on limit equilibrium methods. Japanese Geotechnical Society Special Publication, 2(46), 1632-1635.
[11] De Iorio, A., Grasso, M., Penta, F., Pucillo, G. P., Rossi, S., & Testa, M. (2018). On the ballast–sleeper interaction in the longitudinal and lateral directions. Proceedings of the Institution of Mechanical Engineers, Part F: Journal of Rail and Rapid Transit, 232(2), 620-631.
[12] Shi, C., Fan, Z., Connolly, D. P., Jing, G., Markine, V., & Guo, Y. (2023). Railway ballast performance: recent advances in the understanding of geometry, distribution and degradation. Transportation Geotechnics, 101042.
[13] Shi, C., Zhao, C., Zhang, X., & Guo, Y. (2021). Coupled discrete-continuum approach for railway ballast track and subgrade macro-meso analysis. International Journal of Pavement Engineering, 22(13), 1744-1759.
[14] Fu, L., Zheng, Y., Qiu, Y., & Zhou, S. (2023). Inconsistent effect of dynamic load waveform on macro-and micro-scale responses of ballast bed characterized in individual cycle: a numerical study. Railway Engineering Science, 31(4), 370-380.
[15] Liu, J., Chen, R., Liu, Z., Liu, G., Wang, P., & Wei, X. (2021). Comparative analysis of resistance characteristics of composite sleeper and concrete sleeper in ballast bed. Construction and Building Materials, 300, 124017.
[16] Jing, G., Jia, W., Wang, X., Markine, V., Nålsund, R., & Guo, Y. (2021). Experimental and numerical study on lateral resistance of frictional sleeper with arrowhead groove. Transportation Geotechnics, 30, 100638.
[17] Guo, Y., Fu, H., Qian, Y., Markine, V., & Jing, G. (2020). Effect of sleeper bottom texture on lateral resistance with discrete element modelling. Construction and Building Materials, 250, 118770.
[18] Esmaeili, M., Khodaverdian, A., Neyestanaki, H. K., & Nazari, S. (2016). Investigating the effect of nailed sleepers on increasing the lateral resistance of ballasted track. Computers and Geotechnics, 71, 1-11.
[19] Hosseini, A., & Esmaeili, M. (2017). Effect of different contact surfaces between concrete sleeper and ballast on mobilized lateral resistance against impact loads. Proceedings of the Institution of Mechanical Engineers, Part F: Journal of Rail and Rapid Transit, 231(6), 678-689.
[20] Ngamkhanong, C., Feng, B., Tutumluer, E., Hashash, Y. M., & Kaewunruen, S. (2021). Evaluation of lateral stability of railway tracks due to ballast degradation. Construction and Building Materials, 278, 122342.

[21] Esmaeili, M., Nouri, R., & Yousefian, K. (2017). Experimental comparison of the lateral resistance of tracks with steel slag ballast and limestone ballast materials. Proceedings of the Institution of Mechanical Engineers, Part F: Journal of Rail and Rapid Transit, 231(2), 175-184.
[22] Esmaeili, M., Heydari-Noghabi, H., & Sayadi, A. (2018). Field investigation on the lateral resistance of railway tracks including hot mix asphalt layer. Road Materials and Pavement Design, 19(1), 154-166.
[23] Woodward, P. K., Kennedy, J., Medero, G. M., & Banimahd, M. (2012). Maintaining absolute clearances in ballasted railway tracks using in situ three-dimensional polyurethane geocomposites. Proceedings of the Institution of Mechanical Engineers, Part F: Journal of Rail and Rapid Transit, 226(3), 257-271.
[24] Ling, X., Xiao, H., & Jin, F. (2021). Investigating the effect of different bonding areas on the lateral resistance of polyurethane-mixed ballast using the discrete element method. Proceedings of the Institution of Mechanical Engineers, Part F: Journal of Rail and Rapid Transit, 235(2), 133-142.
[25] Xiao, H., and L. Xing. (2017). Experiment and DEM analysis of lateral resistance of glued ballast. Journal of Southwest Jiaotong University. 52.6.
[26] Xu, L., Zhao, Y., Li, Z., Shi, C., & Yu, Z. (2020). Three-dimensional vehicle-ballasted track-subgrade interaction: Model construction and numerical analysis. Applied Mathematical Modelling, 86, 424-445.
[27] Itasca Consulting Group, Inc, (2014). Particle flow code in 3 dimensions, Minneapolis, 2014.
[28] Tutumluer, E., Qian, Y., Hashash, Y. M., Ghaboussi, J., & Davis, D. D. (2013). Discrete element modelling of ballasted track deformation behaviour. International Journal of Rail Transportation, 1(1-2), 57-73.
[29] Indraratna, B., Ngo, N. T., Rujikiatkamjorn, C., & Vinod, J. S. (2014). Behavior of fresh and fouled railway ballast subjected to direct shear testing: discrete element simulation. International Journal of Geomechanics, 14(1), 34-44.
[30] National Railway Administration of P.R. China. (2017). Code for design of railway track. TB 10082-2017E. Beijing: China Railway Publishing.
[31] National Railway Administration of P.R. China. (2014). Code for design of high speed railway. TB 1062-2014, Beijing: China Railway Publishing.
[32] Suhr, B., Butcher, T. A., Lewis, R., & Six, K. (2020). Friction and wear in railway ballast stone interfaces. Tribology International, 151, 106498.
[33] Chalabii, J., Movahedi Rad, M., Hadizadeh Raisi, E., & Esfandiari Mehni, R. (2022). Effect of Sleeper-Ballast Particle Contact on Lateral Resistance of Concrete Sleepers in Ballasted Railway Tracks. Materials, 15(21), 7508.
[34] Suhr, B., & Six, K. (2017). Parametrisation of a DEM model for railway ballast under different load cases. Granular matter, 19(4), 64.
[35] Tolomeo, M., & McDowell, G. R. (2022). Modelling real particle shape in DEM: a comparison of two methods with application to railway ballast. International Journal of Rock Mechanics and Mining Sciences, 159, 105221.
[36] Xiao, J. L., Liu, G. Z., Liu, J. X., Dai, J. C., Liu, H., & Wang, P. (2019). Parameters of a discrete element ballasted bed model based on a response surface method. Journal of Zhejiang University-SCIENCE A, 20(9), 685-700.
[37] Zakeri JA and Bakhtiary A (2014). Comparing lateral resistance to different types of sleeper in ballasted railway tracks. Scient Iran A; 21: 101–107.

[38] Le Pen, L., Bhandari, A. R., & Powrie, W. (2014). Sleeper end resistance of ballasted railway tracks. Journal of Geotechnical and Geoenvironmental Engineerin